Numerical investigation of film thickness and wave statistics in gas-liquid downwards annular flows

Nicolò Varallo [a], Giorgio Besagni [a], Riccardo Mereu [a]
[a] Politecnico di Milano, Department of Energy, Milano, Italy - e-mail: nicolo.varallo@polimi.it

Abstract

We present a computational fluid dynamics model based on the volume of fluid method for simulating annular gas-liquid flows, focusing on the regular wave flow regime. We performed transient simulations on a 3-D domain using a commercial code (ANSYS Fluent 2021 R1). The mesh sensitivity analysis indicates that a very fine mesh must be used near the pipe wall to capture the liquid-gas interface correctly. The code is validated through available experimental data [1] regarding topological flow properties. In particular, we considered mean film thickness, film roughness, base film thickness, and wave film thickness. We studied two operating conditions. The first is characterized by liquid and gas Reynolds numbers of 1 250 and 25 000, respectively. The second has the same liquid Reynolds number as the first, but the gas Reynolds number is increased to 30 000. The numerical values of the quantities analyzed are in good agreement with the experimental findings, with a maximum error of 21.02% concerning the wave film thickness. The errors regarding the mean film thickness and film roughness are less than 10% for both the case studies.

Numerical model

This study uses the **VOF** approach to model the two immiscible phases, air and water. In the VOF method, in addition to the conservation equations for mass and momentum (Eq. (2) and Eq. (3)), one solves an equation for the filled fraction of phase n in each control volume, α_n, so that $\alpha_n = 1$ in filled controlled volumes and $\alpha_n = 0$ in empty control volumes (Eq. 1). The RNG $k - \varepsilon$ model with enhanced wall functions was chosen to describe the effect of turbulence. To improve turbulence modelling near the gas-liquid interface, the ε-equation has been modified by adding a source term to account for the wall-like damping of turbulence near the interface. The damping source term was calculated using the approach proposed by Egorov [2] (Eq. 3).

$$\frac{\partial \alpha_n}{\partial t} + \nabla \cdot (\alpha_n \boldsymbol{v}) = -\nabla \cdot \left[\gamma |\boldsymbol{v}| \frac{\nabla \alpha_n}{|\nabla \alpha_n|} \alpha_n (1-\alpha_n)\right] \quad \text{Eq. (1)}$$

$$\frac{\partial \rho}{\partial t} + \nabla \cdot (\rho \boldsymbol{v}) = 0 \quad \text{Eq. (2)}$$

$$\frac{\partial}{\partial t}(\rho \boldsymbol{v}) + \nabla \cdot (\rho \boldsymbol{v}\boldsymbol{v}) = -\nabla p + \nabla \cdot (\bar{\bar{\tau}} + \bar{\bar{\tau}}_t) + \rho \boldsymbol{g} + \sigma_{ij} \frac{\rho \boldsymbol{k}_i \nabla \alpha_i}{\frac{1}{2}(\rho_i + \rho_j)} \quad \text{Eq. (3)}$$

$$S_{\varepsilon,i} = \frac{A_i \Delta n C_\mu \rho_i}{k_i} \left(\frac{6 B \mu_i k_i}{\rho_i \Delta n^2}\right)^2 \quad \text{Eq. (4)}$$

Criteria	Setting
Pressure-velocity coupling	PISO
Surface tension model	Continuous surface force with wall adhesion, contact angle 120°
Wall treatment	Enhanced wall functions
Pressure interpolation	Modified body-force weighted
Surface tracking	Geo-reconstruction
Momentum, k, ε discretization	Second order upwind scheme
Transient formulation	First order implicit
Time step	Adaptive with $\mathrm{CFL} < 0.75$ condition
Solution method	Non-iterative time advancement (NITA), conservative with instability detection

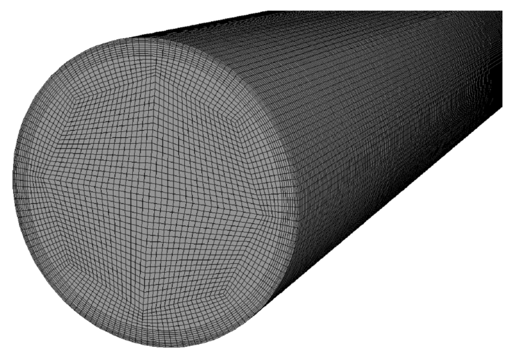

3-D mesh

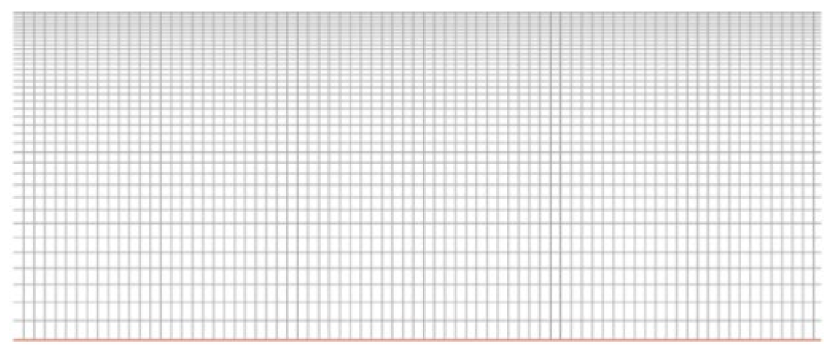

2-D mesh

Case	Re_G	Re_L	Flow regime
A	25 000	1 250	Regular wave
B	30 000	1 250	Regular wave

Results

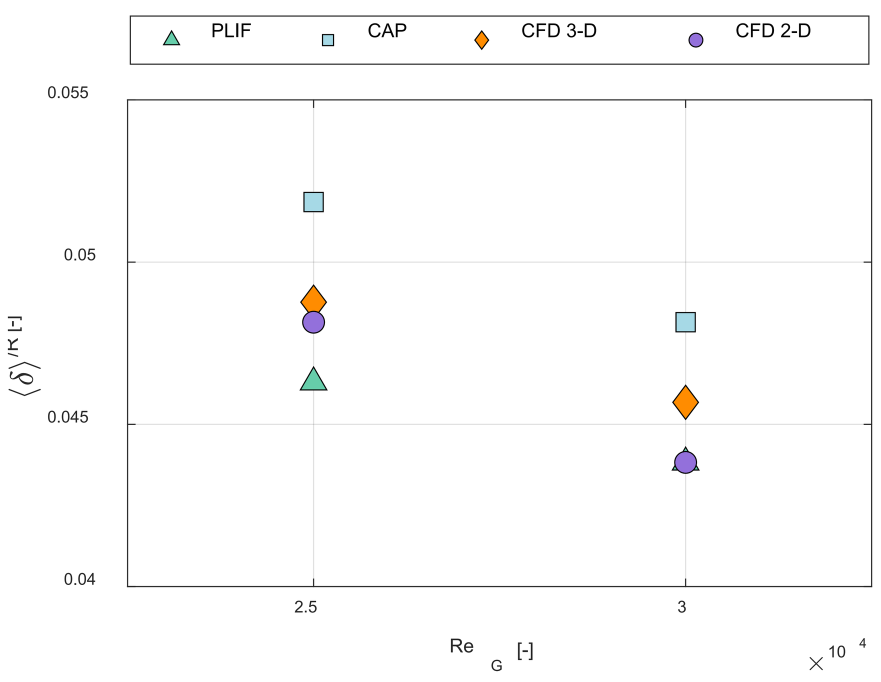

Mean film-thickness

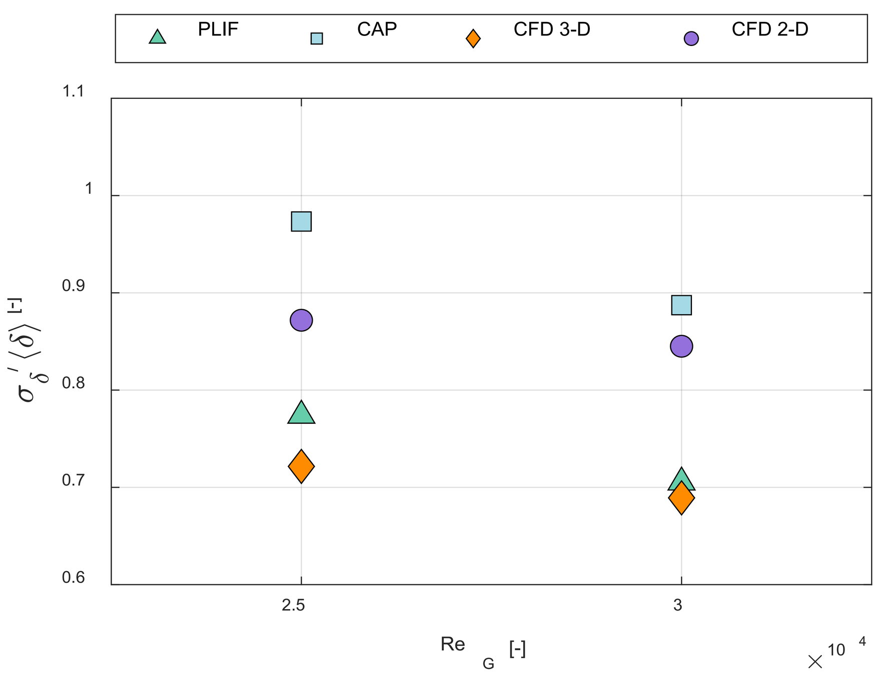

Film roughness

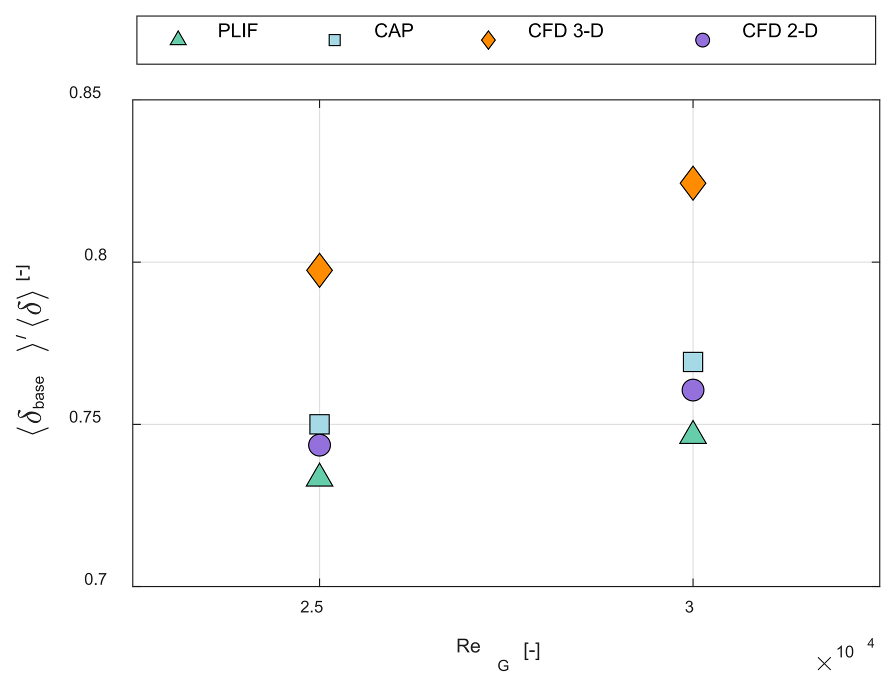

Base film thickness

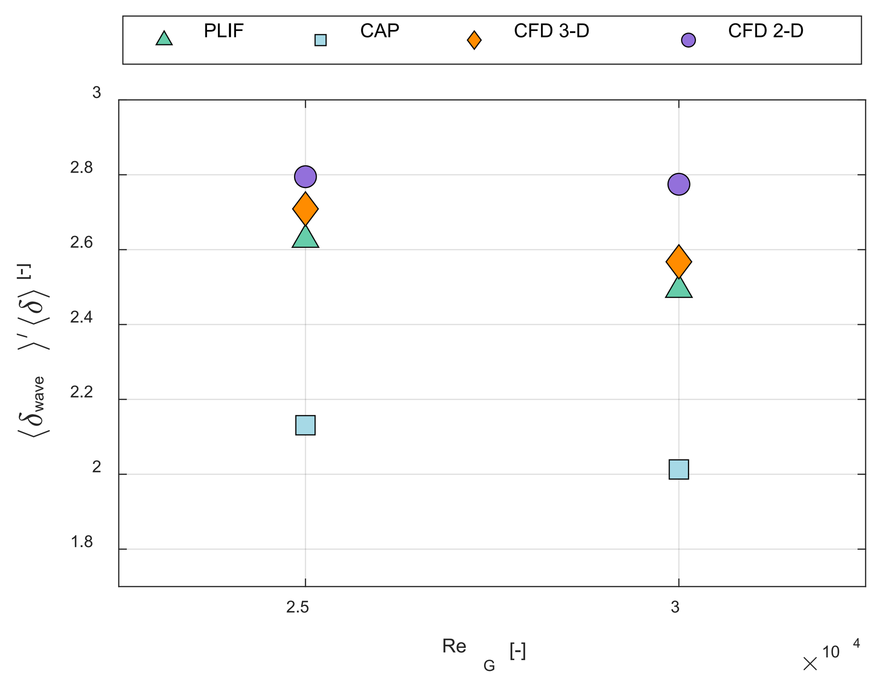

Wave film thickness

Case A

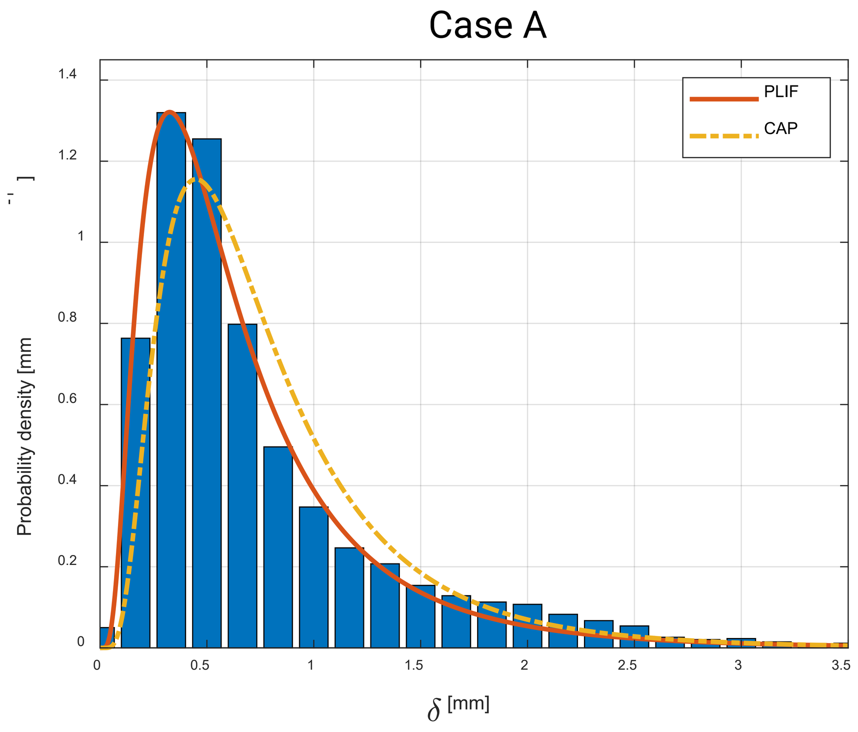

Case B

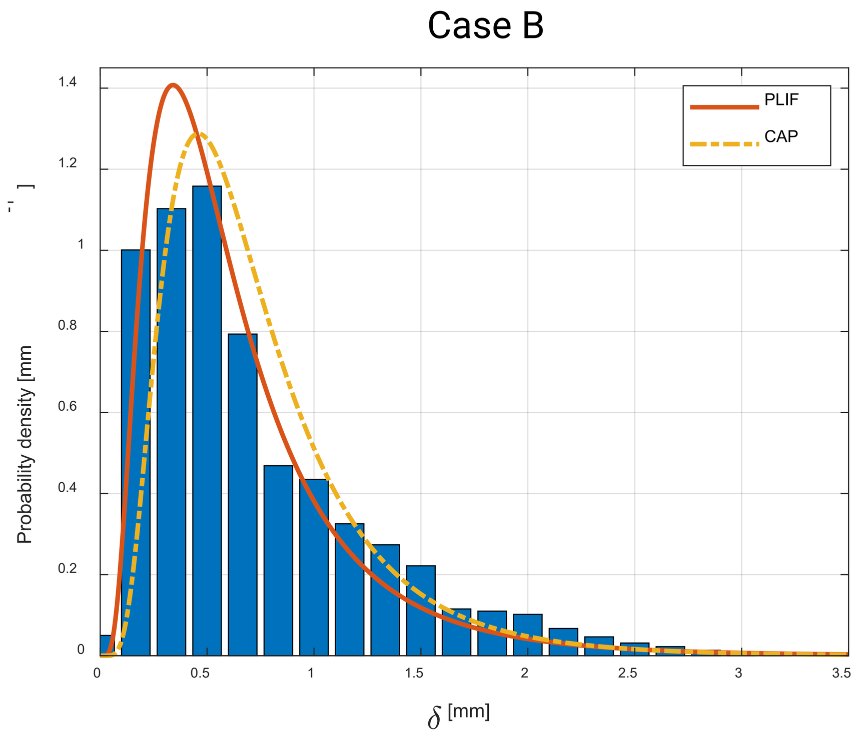

Comparison between the probability density distributions obtained from the numerical results and the experimental PDFs.

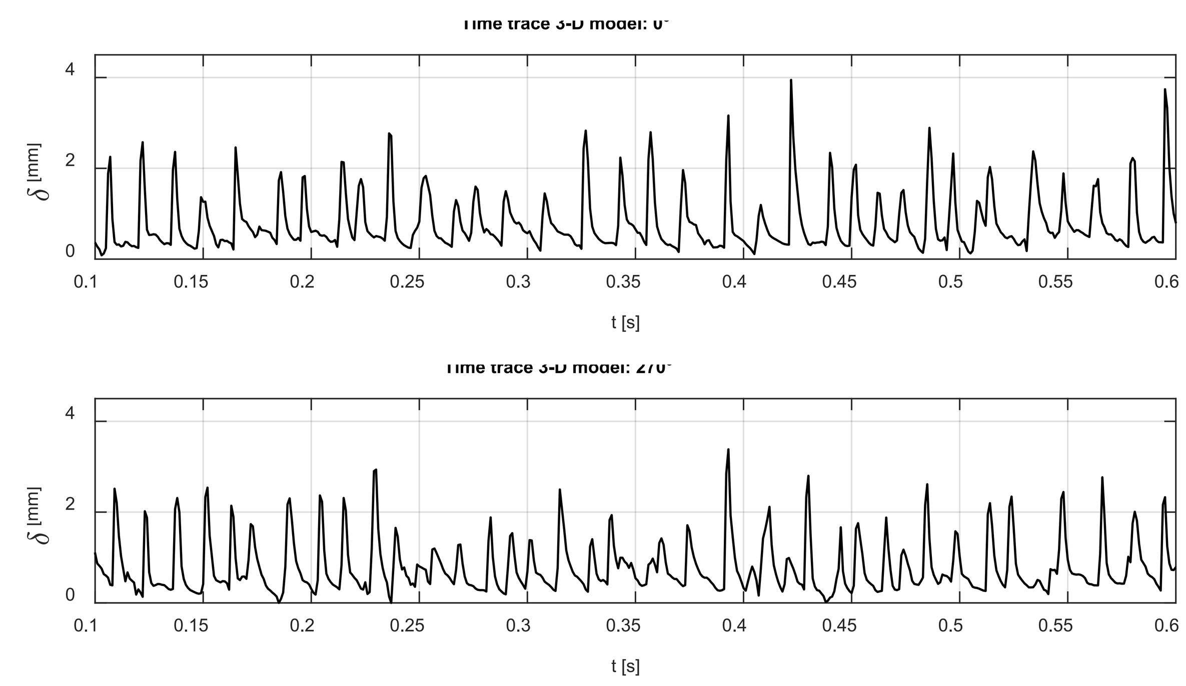

Time traces of film thickness at two circumferential position.

Considering the time traces at different circumferential positions, the cross-correlation coefficients between them have been calculated to determine the presence of circumferential coherent waves. The results are presented in the tables. The high value of the cross-correlation coefficients indicates the presence of coherent waves over the circumference of the pipe, following the experimental results.

Case A

	30°	90°	150°	210°	270°	330°
30°	1	0.70	0.64	0.65	0.65	0.68
90°	-	1	0.70	0.69	0.68	0.72
150°	-	-	1	0.75	0.66	0.67
210°	-	-	-	1	0.68	0.67
270°	-	-	-	-	1	0.70
330°	-	-	-	-	-	1

Case B

	30°	90°	150°	210°	270°	330°
30°	1.00	0.64	0.68	0.65	0.61	0.70
90°	-	1.00	0.71	0.68	0.67	0.72
150°	-	-	1.00	0.70	0.65	0.72
210°	-	-	-	1.00	0.69	0.69
270°	-	-	-	-	1.00	0.72
330°	-	-	-	-	-	1.00

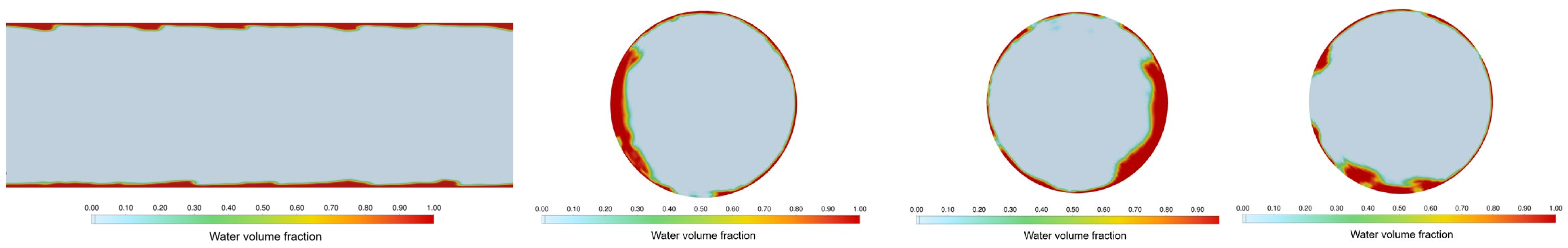

$t = t_0$ [s] $t = t_0 + 0.5$ [s] $t = t_0 + 1.225$ [s]

The 3-D model revels that flow is characterised by a strong instantaneous asymmetry related to the presence of waves with large amplitude not coherent over the pipe circumference. Consequently, the axisymmetric condition is not applicable to the cases studied.

[1] Voulgaropoulos, V., Patapas, A., Lecompte, S ., Charoginnis, A., Matar, O.K., De Paepe, M., Markides, C.N., 2021. Simultaneous laser-induced fluorescence and capacitance probe measurement od downwards annular gas-liquid flows. *Int. J. Multiph. Flow* 142, 103665.
[2] Egorov, Y., 2004. Contact Condensation in Stratified Steam-Water Flow. *EVOL-ECORDA-D 07* .